THE EFFECT OF ARTEMISININ ON THE pH OF *Plasmodium falciparum* DIGESTIVE VACUOLE

NADIAH BINTI IBRAHIM

UNIVERSITI SAINS MALAYSIA

2020

THE EFFECT OF ARTEMISININ ON THE pH OF *Plasmodium falciparum* DIGESTIVE VACUOLE

by

NADIAH BINTI IBRAHIM

Thesis submitted in fulfillment of the requirements

for the degree of

Master of Science

June 2020

ACKNOWLEDGEMENT

Alhamdulillah, all praises to Allah for His blessing and the strengths given to me for completing my MSc. study. First and foremost, I would like to express my utmost gratitude to my main supervisor, Dr. Nurhidanatasha Abu Bakar for her sincere, patience and times that she has spent on me throughout my MSc. journey. Without her guidance and persistent help, this dissertation would not have been possible and I am extremely indebted to her. My appreciation also extends to my co-supervisor, Dr. Maryam Azlan for always giving a bundle of useful advices and knowledge throughout the study. I would also like to acknowledge the lecturers in Institute for Molecular Medicine (INFORMM) especially Dr. Khairul Mohd Fadzli Mustaffa for his generosity providing the parasite samples, sharing the facilities and equipment of parasite culture during my study. Special thanks to the staff in INFORMM, Immunology Department of School of Medical Sciences, Central Research Lab, and School of Health Sciences for giving out full cooperation during the research. A warm appreciation to the past and current members of NAB group especially to Hafizah, Imam and Fatin, which have contributed immensely in this project. Sincere thanks to my friends Hidayah, Bibi, Fatihah, Zakiyyah and Syahidah for the friendships and memories throughout 3 years I have been in USM. But most importantly, none of this could have happened without the support and cares from my family especially my parents, Ibrahim Pa'adik and Rusnani Ismail. They have been really supportive and keep on motivating me to finish my study. Last but not least, my deepest gratitude to USM Graduate Assistant Scheme for providing me the financial support since my 2nd Semester to 4th Semester (2018-2019) and USM Short Term Grant (304/PPSK/61313165) as the research project funding.

TABLE OF CONTENTS

ACKNOWLEDGEMENT ..... **ii**

TABLE OF CONTENTS ..... **iii**

LIST OF TABLES ..... **ix**

LIST OF FIGURES ..... **x**

LIST OF SYMBOLS, ABBREVIATIONS AND ACRONYMNS ..... **xiv**

ABSTRAK ..... **xix**

ABSTRACT ..... **xxi**

CHAPTER 1: INTRODUCTION **1**

1.1 Background of the study 1

1.2 Rationale of the study 4

1.3 Objectives of the study 6

1.3.1 General objective 6

1.3.2 Specific objectives 6

1.4 Experimental design 6

CHAPTER 2: LITERATURE REVIEW **10**

2.1 Overview of malaria 10

2.2 Distribution of malaria 10

2.3 Human malaria parasites 11

2.4 Life cycle of the malaria parasite 14

2.4.1 Sexual cycle of the malaria parasite within a mosquito 14

2.4.2 Asexual cycle of the malaria parasite within a human 16

2.5 Haemoglobin metabolism within the malaria parasite 20
2.5.1 Haemoglobin ingestion by the malaria parasite 20
2.5.2 Haemoglobin transport to the digestive vacuole 22
2.5.2(a) The digestive vacuole of the malaria parasite 23
2.5.3 Haemoglobin digestion in the digestive vacuole 24
2.5.3(a) Maintenance of the digestive vacuole pH 26
2.5.3(b) Detoxification of haem and haematin in the digestive vacuole 29
2.6 Clinical manifestation of malaria 30
2.7 Diagnosis of malaria 31
2.8 Treatment of malaria 32
2.8.1 Past antimalarial drugs 34
2.8.2 Current antimalarial drugs 35
2.9 Artemisinin 36
2.9.1 Mechanism of activation of artemisinin 38
2.9.2 Mechanism of action of artemisinin 40
2.10 Measurement of the pH of the digestive vacuole 42
2.10.1 Ratiometric pH-sensitive fluorescent probes 43
2.11 The 4-hour drug pulse assay 45
2.11.1 Malaria SYBR Green I-based fluorescence (MSF) assay 46

CHAPTER 3: MATERIALS AND METHODS 47

3.1 Malaria parasite culturing methods 47
3.1.1 Malaria parasite strain 47
3.1.2 Thawing of cryopreserved malaria parasite-infected erythrocytes 47

3.1.3 *In vitro* culture of malaria parasite-infected erythrocytes 48
3.1.4 Sub-culture of malaria parasite-infected erythrocytes 48
3.1.5 Determination of parasitaemia and parasite stage 49
3.1.6 Synchronisation of ring stage parasite-infected erythrocytes 52
3.1.7 Enrichment and purification of mature stage parasite-infected erythrocytes 52
3.2 Preparation of resealed erythrocytes containing fluorescent probes 53
3.2.1 Preparation of fluorescent probe stock solutions 53
3.2.2 Measurement of fluorescent probe stock solution concentrations 55
3.2.3 Resealing of erythrocytes containing fluorescent probes 55
3.2.3(a) Imaging of resealed erythrocytes containing fluorescent probes 57
3.2.3(b) Identification of the resealed erythrocyte population containing FITC-dextran 58
3.2.4 Determination of the optimal loading concentration of FITC-dextran 58
3.3 Culture of malaria parasites with resealed erythrocytes containing FITC-dextran 59
3.4 Selective permeabilisation of the erythrocyte plasma membrane and the parasitophorous vacuolar membrane 61
3.4.1 Preparation of saponin stock solutions 61
3.4.2 Determination of the optimal permeabilising concentration of saponin 61
3.5 Preparation of a pH calibration curve of FITC-dextran using saponin-permeabilised parasites 63

3.5.1 Flow cytometry analysis of saponin-permeabilised parasites for generation of a pH calibration curve 64
3.5.2 Measurement of the digestive vacuole pH using a pH calibration curve of FITC-dextran 64
3.6 Measurement of the digestive vacuole pH after 4-hour artemisinin pulse 65
3.6.1 Preparation of artemisinin and SYBR Green I stock solutions 65
3.6.2 Gating of different developmental stages of parasites stained with SYBR Green I 66
3.6.3 The 4-hour artemisinin pulse assay 66
3.6.3(a) Preparation of drug and parasite plates 67
3.6.3(b) Determination of the 4-hour pulse inhibitory concentration 50% ($IC_{50\text{-}4\ hours}$) and sub-lethal concentrations of artemisinin 70
3.6.4 Measurement of the digestive vacuole pH after 4-hour pulse with sub-lethal concentrations of artemisinin 72

CHAPTER 4: RESULTS 75

4.1 Characterisation of resealed erythrocytes containing fluorescent probes 75
4.1.1 Spectrophotometric measurement of fluorescent probe primary stock concentrations 75
4.1.2 Morphology of resealed erythrocytes after resealing process 78
4.1.3 Scatter and fluorescence intensity profiles of the FITC-dextran-containing resealed erythrocyte population 82
4.1.4 The optimal loading concentration of FITC-dextran in resealed erythrocytes 84

4.1.5 Invasion efficiency of resealed erythrocytes with FITC-dextran by *P. falciparum* 86

4.1.6 The transport of FITC-dextran into the parasite's digestive vacuole ... 89

4.2 Characterisation of saponin-permeabilised parasites containing FITC-dextran 92

4.2.1 The optimal concentration of saponin for permeabilisation process 92

4.2.2 The gating strategy for determination of the saponin-permeabilised parasite population 93

4.2.3 The accumulation of FITC-dextran in the digestive vacuole of saponin-permeabilised parasites 99

4.2.4 FITC-dextran as a pH indicator in saponin-permeabilised parasites .. 101

4.3 The pH of the digestive vacuole after 4-hour artemisinin pulse..... 104

4.3.1 Flow cytometry analysis for determination of the $IC_{50\text{-}4\ hours}$ and sub-lethal concentrations of artemisinin 104

4.3.1(a) The SYBR Green I staining differentiates the populations between ring and trophozoite stage parasites 105

4.3.1(b) The short 4-hour artemisinin pulse affected the parasite growth and viability 108

4.3.2 Sub-lethal concentrations of artemisinin altered the digestive vacuole pH 114

CHAPTER 5: DISCUSSION 119

5.1 FITC-dextran-containing resealed erythrocytes: a model for the study of the digestive vacuole pH measurement 119

5.2 Sub-lethal concentrations of artemisinin determined by using the 4-hour drug pulse assay delay the parasite growth..... 123

5.3 Sub-lethal concentrations of artemisinin alter pH of the digestive vacuole ... 126

5.4 Artemisinin inhibits the V-type H^+-ATPase activity that in turn increases the digestive vacuole pH: a postulation of the mechanism of action of artemisinin 127

CHAPTER 6: CONCLUSION..... 130

REFERENCES..... 132

APPENDICES

Appendix A Human ethical approval

Appendix B Subject information and consent form

LIST OF PRESENTATIONS AND PUBLICATIONS

LIST OF TABLES

		Page
Table 3.1	Volumes of CCM and total blood required for maintaining the parasite in culture flasks at different haematocrits	50

LIST OF FIGURES

		Page
Figure 1.1	Flowchart of the experiments through all the study	9
Figure 2.1	The malaria incidence rates worldwide from 2000-2017	12
Figure 2.2	The number of malaria cases in Malaysia from 2005-2017	13
Figure 2.3	The sexual cycle of the malaria parasite within a mosquito	15
Figure 2.4	The asexual cycle of the malaria parasite within a human	17
Figure 2.5	The intraerythrocytic stages of *P. falciparum*	19
Figure 2.6	The schematic diagram of haemoglobin ingestion, transport to and digestion in the digestive vacuole of *P. falciparum*	21
Figure 2.7	The formation of haemozoin in the digestive vacuole	25
Figure 2.8	The schematic diagram of the proton pumps at the digestive vacuole's membrane	28
Figure 2.9	The chemical structure of the antimalarial drugs	33
Figure 2.10	The chemical structure of artemisinin and its derivatives	37
Figure 2.11	The schematic diagram of the proposed pathways of activation of artemisinin	39
Figure 2.12	The molecular structure of fluorescein in different prototropic forms	44
Figure 3.1	Asexual developmental stages of *P. falciparum* throughout the 48 hours intraerythrocytic life cycle	51
Figure 3.2	Enrichment and purification of mature stage parasite-infected erythrocytes by using the magnetic cell separation technique	54
Figure 3.3	Resealing method for the entrapment of fluorescent probes in resealed erythrocytes	56

Figure 3.4	A schematic diagram of the uptake and transport of haemoglobin and FITC-dextran to the digestive vacuole of the malaria parasite within a resealed erythrocyte	60
Figure 3.5	A schematic diagram of a saponin-permeabilised erythrocyte infected with a trophozoite stage parasite	62
Figure 3.6	Schematic protocols for 4-hour artemisinin pulse assays	68
Figure 3.7	Preparation of two-fold serial dilutions of artemisinin in a 96-well microplate	69
Figure 3.8	Preparation of parasite suspensions for 4-hour artemisinin pulse assays	71
Figure 3.9	Schematic protocols for pH measurement of the digestive vacuole of parasites pulsed with sub-lethal concentrations of artemisinin for 4 hours	74
Figure 4.1	The absorption spectrum of FITC-dextran	76
Figure 4.2	The measurement of the FITC-dextran concentration using the Beer-Lambert equation	77
Figure 4.3	The absorption spectrum of TMR-dextran	79
Figure 4.4	The measurement of the TMR-dextran concentration using the Beer-Lambert equation	80
Figure 4.5	The resealed erythrocytes containing fluorescent probes	81
Figure 4.6	The scatter plot and fluorescence intensity histograms of resealed erythrocytes containing FITC-dextran	83
Figure 4.7	The optimisation of FITC-dextran loading concentrations in resealed erythrocytes	85
Figure 4.8	The erythrocytes resealed with different loading	87

concentrations of FITC-dextran

Figure 4.9 The invasion index of the malaria parasite with different types of erythrocytes 88

Figure 4.10 The growth of ring stage parasites in different types of erythrocytes 90

Figure 4.11 The uptake and transport of FITC-dextran into the parasite's digestive vacuole 91

Figure 4.12 The flow cytometry analysis of uninfected resealed erythrocytes containing FITC-dextran after saponin permeabilisation 94

Figure 4.13 The number of remaining resealed erythrocytes with FITC-dextran after permeabilisation with different concentrations of saponin 95

Figure 4.14 The gating strategy for determination of the population of saponin-permeabilised parasites in non-resealed erythrocytes 97

Figure 4.15 The gating strategy for determination of the population of saponin-permeabilised parasites in resealed erythrocytes containing FITC-dextran 98

Figure 4.16 The accumulation of FITC-dextran in the digestive vacuole of trophozoite stage parasites after saponin permeabilisation 100

Figure 4.17 The pH calibration curves of FITC-dextran in different pH buffers in the presence of an ionophore, CCCP 102

Figure 4.18 The fluorescence ratios (R_{gy}) of saponin-permeabilised parasites after treatment with a proton pump inhibitor, concanamycin A 103

Figure 4.19	The negative controls in the SYBR Green I staining of infected erythrocytes	106
Figure 4.20	The SYBR Green I staining of erythrocytes infected with ring and trophozoite stage parasites	107
Figure 4.21	The SYBR Green I analysis of parasites treated with different concentrations of artemisinin in the 4-hour pulse observed at 24- and 48-hour post-treatments	109
Figure 4.22	The 4-hour artemisinin pulse assay produces different parasite populations	110
Figure 4.23	The SYBR Green I staining profiles of parasites treated with different concentrations of artemisinin at 24-hour post-treatment	112
Figure 4.24	The morphology of *P. falciparum* pulsed for 4 hours with artemisinin	113
Figure 4.25	Sub-lethal concentrations of artemisinin delayed the parasite growth	116
Figure 4.26	Sub-lethal concentrations altered the digestive vacuole pH	118

LIST OF SYMBOLS, ABBREVIATIONS AND ACRONYMNS

~	approximately
%	percent
°C	degree Celsius
Ɛ	molar absorptivity
±	plus minus
<	less than
≤	less than or equal to
>	more than
≥	more than or equal to
µM	micromolar
nM	nanomolar
mM	millimolar
µl	microliter
mL	mililiter
mg	milligram
g	gram
cm	centimetre
nm	nanometre
× *g*	gravitational force
ACTs	artemisinin-based combination therapies
ADP	adenosine diphosphate
AMDP	aminomethylenediphosphonate
ANOVA	analysis of variance

ATP	adenosine triphosphate
BFMP	blood film for malaria parasite
BCECF	5'(and 6')-carboxy-10- dimethylamino-3-hydroxy-spiro[7H-benzo[c] xanthene-7,1'(3H)-isobenzofuran]-3'-one
CCM	complete culture medium
CCCP	carbonyl cyanide m-chlorophenylhydrazone
df	dilution factor
DNA	deoxyribonucleic acid
DMSO	dimethyl sulfoxide
DV	digestive vacuole
ECM	endocytosis medium
e.g.	for example
E-64	a specific inhibitor of cysteine protease
EPM	erythrocyte plasma membrane
ES	extracellular saline
ETC	electron transport chain
FACS	fluorescence-activated cell sorting
FCS	Flow Cytometry Standard
Fe	iron
Fe(II)	ferrous iron
Fe(III)	ferric iron
FPFe(II)	ferroprotoporphyrin IX
FPFe(III)	ferriprotoporphyrin IX
FITC	fluorescein isothiocyanate

FSC	forward scatter
GSH	(2*S*)-2-Amino-4-{[(1*R*)-1-[(carboxymethyl)carbamoyl]-2-sulfanylethyl]carbamoyl}butanoic acid
Hb	haemoglobin
HEPES	hydroxyethyl piperazineethanesulfonic acid
HRPII	histidine-rich protein II
H_2O_2	hydrogen peroxide
H^+	hydrogen ion
$IC_{50\text{-}4\ hours}$	4-hour pulse inhibitory concentration 50%
ICCM	incomplete culture medium
i.e.	that is
I_g	fluorescence intensity collected at green channel
I_y	fluorescence intensity collected at yellow channel
IDP	imidodiphosphate
IL-1β	interleukin-1β
K^+	potassium ion
KCl	potassium chloride
L	lethal concentration
MACS	magnetic-activated cell sorting
MES	2-[N-morpholino] ethane sulfonic acid
MSF	malaria SYBR Green I-based fluorescence
Mg^{2+}	magnesium ion
MgCl	magnesium chloride
NaCl	sodium chloride

NaF	sodium fluoride
NaH_2PO_4	sodium phosphate
NLRP3	NOD-like receptor containing pyrin domain 3
n.d	no drug
PCR	polymerase chain reaction
PE	phycoerythrin
*Pf*ATP6	*Plasmodium falciparum* sacrco/endoplasmic reticulum Ca^{2+}-ATPase
*Pf*PM4	*P. falciparum* digestive vacuole's aspartic protease, plasmepsin IV
pLDH	*Plasmodium* lactate dehydrogenase
pK_a	acid dissociation constant
PP_i	pyrophosphate
PPM	parasite plasma membrane
PV	parasitophorous vacuole
PVM	parasitophorous vacuolar membrane
RDT	rapid diagnostic test
RNA	ribonucleic acid
RPMI	Rosewell Park Memorial Institute
R_{gy}	fluorescence ratio
SNARF	5'(and 6')-carboxy-10- dimethylamino-3-hydroxy-spiro[*7H*-benzo[c] xanthene-7,1'(*3H*)-isobenzofuran]-3'-one
SSC	side scatter
SERCA	sarco/endoplasmic reticulum Ca^{2+}-ATPase

SEM	standard error of mean
SL	sub-lethal concentration
TCTP	translationally controlled tumor protein
TMR-dextran	tetramethylrhodamine-dextran
TLR9	Toll-like receptor 9
TRIS	tris (hydroxymethyl) aminomethane
V-type H^+-ATPase	vacuolar-type proton-pumping ATPase
V-type H^+-pyrophosphate	vacuolar-type proton-pumping pyrophosphatase
WHO	World Health Organization
w/v	weight per volume
-ve	negative control

KESAN ARTEMISININ KE ATAS pH VAKUOL PENCERNAAN *Plasmodium falciparum*

ABSTRAK

Artemisinin merupakan ubat antimalaria yang sangat berkesan dan digunakan secara meluas kerana keupayaannya dalam membunuh parasit *Plasmodium* dengan pantas. Namun, artemisinin telah dilaporkan mempunyai kurang kerentanan terhadap *P. falciparum* di Asia Tenggara menyebabkan permintaan kepada ubat antimalaria baru yang mempunyai cara tindakan serupa dengan artemisinin. Sehingga kini, mekanisme tindakan artemisinin yang tepat masih dipertikaikan walaupun penyelidikan telah dijalankan berdekad lamanya. Bukti terbaru menunjukkan artemisinin mempunyai perencatan terus terhadap pam proton, ATPase-H^+ Jenis-V yang terletak pada membran vakuol pencernaan parasit, di mana perencatan tersebut menyebabkan perubahan pH dalam organel berasid itu. Oleh itu, pH vakuol pencernaan parasit yang dirawat dengan artemisinin diukur dalam kajian ini menggunakan sitometri aliran. Asai berasaskan sitometri aliran telah dioptimumkan untuk mengukur pH vakuol pencernaan menggunakan penunjuk pH bersifat ratiometrik iaitu, fluorescein isothiocyanate-dextran (FITC-dextran) dimuatkan ke dalam vakuol pencernaan parasit. Satu lengkung penentukuran pH dijana dengan menggunakan parasit pada peringkat trofozoit yang dipencilkan dan diampaikan dalam larutan penimbal yang berbeza pH dengan kehadiran ionofor, carbonyl cyanide m-chlorophenylhydrazone (CCCP). Tanpa CCCP, keadaan stabil pH vakuol pencernaan berada pada nilai 5.42 ± 0.11. Seterusnya, aktiviti antimalaria artemisinin dinilai menggunakan asai rawatan selama 4 jam (memimikkan

pendedahan *in vivo*) bagi menentukan kepekatan perencatan sebanyak 50% ($IC_{50\text{-}4\ jam}$) dan kepekatan sub-maut (menyebabkan kematian parasit kurang dari 25%). Parasit pada peringkat cincin pertengahan dirawat menggunakan kepekatan artemisinin yang berbeza (0-10000 nM) selama 4 jam dan dilarutkan dengan media bagi menyingkirkan artemisinin. Kultur parasit terus dikulturkan selama 24 jam untuk pemerhatian terhadap pertumbuhan parasit dan 48 jam untuk memeriksa kebolehhidupan parasit. Kepekatan sub-maut (15 dan 30 nM) dipilih daripada kajian ini untuk memastikan perubahan pH vakuol pencernaan yang dilihat dalam eksperimen seterusnya bukan disebabkan kematian parasit. Dengan menggunakan asai rawatan 4-jam keatas parasit pada peringkat cincin pertengahan, kepekatan sub-maut meningkatkan pH vakuol pencernaan sebanyak 0.49 (15 nM, pH = 5.7 ± 0.1) dan 1.56 unit pH (30 nM, pH = 6.77 ± 0.48), apabila dibandingkan dengan parasit yang tidak dirawat (pH = 5.21 ± 0.04). Asai yang sama juga dilakukan keatas parasit pada peringkat trofozoit pertengahan untuk membolehkan pengukuran terus pH vakuol pencernaan. pH vakuol pencernaan telah meningkat sebanyak 1 (15 nM, pH = 6.6 ± 0.1) dan 1.48 unit pH (30 nM, pH = 7.1 ± 0.08), apabila dibandingkan dengan parasit yang tidak dirawat (pH = 5.6 ± 0.1). Keputusan perubahan pH vakuol pencernaan yang sama disebabkan oleh perencat ATPase-H^+ Jenis-V, concanamycin juga dapat dilihat (pH = 7.4 ± 0.1). Kesimpulannya, keputusan tersebut menunjukkan artemisinin seperti concanamycin A berupaya merencat ATPase-H^+ Jenis-V yang menyebabkan perubahan pH di dalam vakuol pencernaan. Asai berasaskan sitometri aliran dalam kajian ini menyediakan model yang mudah dan tepat untuk pengukuran pH vakuol pencernaan serentak dengan penilaian pertumbuhan parasit dan kebolehhidupan selepas rawatan dengan menggunakan ubat antimalaria yang lain.

THE EFFECT OF ARTEMISININ ON THE pH OF *Plasmodium falciparum* DIGESTIVE VACUOLE

ABSTRACT

Artemisinin, a highly potent antimalarial drug is widely used due to the rapid killing of *Plasmodium* parasites. However, artemisinin has been reported to have reduced susceptibility against *P. falciparum* in Southeast Asia demanding for new antimalarial drugs that have a similar mode of action with artemisinin. To date, the precise mechanism of action of artemisinin remains disputable despite decades of research. Recent evidence showed that artemisinin might have a direct inhibition of proton pump, V-type H^+-ATPase located on the membrane of parasite's digestive vacuole, in which the inhibition causes pH alteration in the acidic organelle. Hence, the pH of the digestive vacuole of parasites treated with artemisinin was measured in this study by using flow cytometry. The flow cytometry-based assay was optimised to measure the digestive vacuole pH using a ratiometric pH indicator, fluorescein isothiocyanate (FITC)-dextran loaded into the parasite's digestive vacuole. A standard pH calibration curve is generated by using the isolated trophozoite stage parasites suspended in buffers with different pH in the presence of an ionophore, carbonyl-cyanide m-chlorophenylhydrazone (CCCP). Without CCCP, the steady-state digestive vacuole pH showed an acidic value of 5.42 ± 0.11. Next, the antimalarial activity of artemisinin was evaluated by using a 4-hour drug pulse assay to determine the 50% inhibitory concentration ($IC_{50\text{-}4\ hours}$) and sub-lethal concentrations (caused less than 25% parasite death). Mid ring stage parasites were pulsed with different concentrations of artemisinin (0-1000 nM) for 4 hours (mimic *in vivo*

exposure) and then washed to remove the drugs. The parasite cultures were continually cultured for 24 hours to examine its growth and 48 hours to examine its viability. Sub-lethal concentrations (15 and 30 nM) were selected from this study to ensure the digestive vacuole pH change observed in the subsequent experiment was not due to parasite death. Using the similar assay of 4-hour drug pulse on mid ring stage parasites, the sub-lethal concentrations increased the digestive vacuole pH by 0.49 (15 nM, pH = 5.7 ± 0.1) and 1.56 pH unit (30 nM, pH = 6.77 ± 0.48), respectively as compared with the untreated parasites (pH = 5.21 ± 0.04). The same assay was performed at mid trophozoite stage parasites to enable direct measurement of the digestive vacuole pH. The pH of the digestive vacuole was increased by 1 (15 nM, pH = 6.6 ± 0.1) and 1.48 pH unit (30 nM, pH = 7.1 ± 0.08), respectively as compared with the untreated parasites (pH = 5.6 ± 0.1). A similar result of the digestive vacuole pH alteration caused by a standard V-type H^+-ATPase inhibitor, concanamycin A was observed (pH = 7.4 ± 0.1). In conclusion, the result showed that artemisinin, like concanamycin A may inhibit the V-type H^+-ATPase, which caused the pH alteration in the digestive vacuole. The flow cytometry-based assay in this study provides a simple and accurate model for the measurement of digestive vacuole pH with a simultaneous evaluation on parasite growth and viability following treatment with other antimalarial drugs.

CHAPTER 1

INTRODUCTION

1.1 Background of the study

Malaria is a global health issue and remains a prominent infectious disease in developing countries especially in tropical and subtropical regions. In 2017, approximately 219 million malaria cases were reported worldwide with an estimated 435 000 deaths (World Health Organization (WHO), 2018). In Malaysia, a total of 508 cases including local and imported cases were recorded in 2017 (WHO, 2018). The influxes of foreign workers especially from malaria endemic countries have contributed to the recurrence of the cases and the widespread of the disease (Yong *et al.*, 2018). Hence, massive efforts and strategies are warranted to eliminate malaria.

Malaria is generally transmitted to humans through the bites of infected female *Anopheles* mosquitoes. The disease can also be transmitted via blood transfusion or sharing needles contaminated with the parasite. There are five species of the human malaria parasites namely *Plasmodium falciparum, P. vivax, P. ovale, P. malariae* and *P. knowlesi*. Among these species, *P. falciparum* is the most virulent and responsible for the highest rate of morbidity and mortality of malaria worldwide (Geleta and Ketema, 2016).

Plasmodium falciparum has a multistage life cycle to complete its growth and development in different hosts (Aly *et al.*, 2009). The sexual cycle of the malaria

parasite occurs in a mosquito, which involves the production of infective sporozoites. The sporozoites enter the human host during the blood feeding, initiating the asexual cycle. The asexual cycle of the parasite involves two main phases; the exoerythrocytic and intraerythrocytic phases. The exoerythrocytic phase begins when the sporozoites enter the bloodstream and invade the hepatocytes. After maturation of live-stage schizonts, thousands of merozoites are released from the bursting of the hepatocytes. The merozoites subsequently invade the erythrocytes, initiating the intraerythrocytic phase. At this phase, the parasite takes approximately 48 hours to complete its pathogenic life cycle, which is responsible for the clinical manifestations of the disease (Josling and Llinás, 2015).

Common clinical symptoms caused by the malaria parasites grown in the erythrocytes are headache, fever, vomiting, muscle pain and diaphoresis. These mild symptoms can progress into severe illness such as severe anaemia and cerebral malaria, which can cause death without immediate and proper treatment (Trampuz *et al.*, 2003; White, 2018). To date, the chemotherapeutic treatment using antimalarial drugs remains the primary option to combat malaria as there is no effective vaccine available thus far (Mahmoudi and Keshavarz, 2017).

Chloroquine, an antimalarial drug from the class of 4-aminoquinolines, was the most prescribed drug for malaria treatment (Al-Bari, 2015). Due to the emergence and spread of parasite populations resistant to this drug, this has led to the discovery of endoperoxide-containing compounds, artemisinin and its derivatives (Rudrapal and Chetia, 2016). These promising drugs have a superior activity against all intraerythrocytic stage parasites (Mohd-Zamri *et al.*, 2017a) and have been used

together with other drugs that have long-lasting effects in artemisinin-based combination therapies (ACTs) (Pinheiro *et al.*, 2018). Currently, ACTs have been recommended as the first-line treatment for uncomplicated malaria (WHO, 2010). Worryingly, the decline in susceptibility of artemisinin against the parasites was reported in Southeast Asia countries such as in Thailand and Cambodia and manifested clinically as longer parasite clearance time (Fairhurst and Dondorp, 2016; Hanboonkunupakarn and White, 2016). Thus, it is important to understand the precise mode of action of artemisinin in a view to reveal the key drug target within the parasite.

The precise mechanism of action of artemisinin is still a matter of debate among researchers over the decades. Although several parasite proteins have been reported to be the drug targets (Wang and Lin, 2016), none of them could satisfactorily account for the rapid and potent inhibitory effect of artemisinin. A recent proteomics study by Wang *et al.* (2015) identified several parasite proteins as the targets of artemisinin including V-type H^+- pyrophosphatase. Another study by Ismail *et al.* (2016), also demonstrated that two subunits A and B of the V-type H^+-ATPase are the targets of artemisinin. V-type H^+-pyrophosphatase and V-type H^+-ATPase have been shown to act together to maintain a low internal pH of the digestive vacuole of the malaria parasite (Hapuarachchi *et al.*, 2017; Saliba *et al.*, 2003). We hypothesised that artemisinin might have a direct effect on the digestive vacuole's proton pumps, thereby causing the alkalinisation of this organelle and eventually the parasite death. The present study was conducted to measure the pH of the digestive vacuole of the parasites treated with artemisinin and its correlation with parasite growth and viability.

1.2 Rationale of the study

The malaria parasite spends part of its life cycle inside the erythrocyte. Using cytostomes, the parasite performs endocytosis to internalise the haemoglobin (Dluzewski *et al.*, 2008; Milani *et al.*, 2015). Budding of the cytostomes leads to the formation of haemoglobin-containing endocytic vesicles (Lazarus *et al.*, 2008). These vesicles are transferred to the digestive vacuole for degradation by proteases (Abu Bakar *et al.*, 2010). Several proteases involved in the haemoglobin degradation are aspartic, cysteine and metalloproteinases that work optimally in the pH ranging from 4.5-5.5 (Liu, 2017b; Na *et al.*, 2010), suggesting that the digestive vacuole maintains an acidic environment.

The maintenance of the acidic pH of the digestive vacuole has been regulated by the action of the proton pumps, V-type H^+-ATPase and V-type H^+-pyrophosphatase located at the digestive vacuole's membrane (Hapuarachchi *et al.*, 2017; Shah *et al.*, 2016). These proton pumps have been responsible to promote the influx of H^+ into the digestive vacuole (Abu Bakar, 2015). The inhibition of V-type H^+-ATPase and V-type H^+-pyrophosphatase by specific inhibitors such as concanamycin A and imidodiphosphate (IDP) respectively caused the alkalinisation of the digestive vacuole (Shah *et al.*, 2016).

The ultrastructural study by del Pilar Crespo *et al.* (2008) using serial thin-section transmission electron microscopy showed that treatment with artemisinin (40 times the IC_{50} values of the drug) for 8 hours caused the disruption of the digestive vacuole's membrane. The authors also observed using fluorescence

microscopy the cellular distribution of the pH probe (LysoSensor Blue) in the digestive vacuole, suggesting an early disruption of the pH gradient. However, it is still obscure whether this was due to the primary action of artemisinin or as the consequence of parasite death due to higher concentration of artemisinin and longer treatment with the drug.

To address the question, in the present study, a flow cytometry-based assay was developed for a quantitative analysis of pH of the digestive vacuole of parasites pulsed for 4 hours with sub-lethal concentrations of artemisinin by using a pH-sensitive fluorescent probe, fluorescein isothiocyanate (FITC)-dextran. Flow cytometry offers an alternative technique for evaluating pH changes of the digestive vacuole on a population of erythrocytes and permits direct correlation with parasite growth (Abu Bakar, 2015; Ibrahim and Abu-Bakar, 2019). A DNA/RNA-binding fluorescent dye, SYBR Green I that takes advantage of the absence of nucleic acids in mature erythrocytes was used with flow cytometry to discriminate between infected and uninfected erythrocytes. This significantly facilitates direct and correlative measurements between multiple parameters, which are digestive vacuole pH and parasite growth and survival. Parasites were exposed to a short 4-hour pulse with different concentrations of artemisinin to mimic the duration of clinical exposure to the drug, which has a short half-life. The 4-hour pulse inhibitory concentration 50% ($IC_{50\text{-}4\ hours}$) and the sub-lethal concentrations of the drug that caused less than 25% parasite death were determined and employed throughout subsequent experiments. The study might be able to explain the action and specificity of artemisinin in parasite killing and facilitate the development of better strategies to treat malaria in times of emerging resistance to artemisinin.

1.3 Objectives of the study

1.3.1 General objective

To determine pH changes of the digestive vacuole of the chloroquine-sensitive (3D7) strain of *P. falciparum* treated with sub-lethal concentrations of artemisinin in the 4-hour pulse drug inhibition assay

1.3.2 Specific objectives

i. To determine optimal loading concentration of FITC-dextran in resealed erythrocytes
ii. To generate a standard pH calibration curve using saponin-permeabilised parasites containing FITC-dextran
iii. To determine the 4-hour pulse inhibitory concentration 50% ($IC_{50\text{-}4\ hours}$) and sub-lethal concentrations of artemisinin against mid ring stage parasites.
iv. To measure the pH of the digestive vacuole of the parasite pulsed for 4 hours with sub-lethal concentrations of artemisinin and its correlation with parasite growth

1.4 Experimental design

The aim of the study was to measure the pH of the digestive vacuole of the malaria parasite pulsed for 4 hours with sub-lethal concentrations of artemisinin. The digestive vacuole pH was measured using a ratiometric pH indicator, FITC-

dextran incorporated into resealed erythrocytes using a method of hypotonic haemolysis dilution. Beforehand, an optimal loading concentration of FITC-dextran was determined to detect sufficient fluorescence signal while minimising the loss of haemoglobin during the resealing process. Ring stage parasites were treated with sorbitol to obtain a synchronous population of mature stage parasites at 26-hour post-synchronisation. Mature stage parasites were harvested using a magnetic column separation technique and cultured with resealed erythrocytes.

The invasion of early ring stage parasites in resealed erythrocytes was observed at 14-hour post-inoculation (~6-hour post-invasion). After 42-hour post-inoculation (~34-hour post-invasion), trophozoite stage parasites with accumulated FITC-dextran within the digestive vacuole were isolated by brief exposure with 0.035% (w/v) saponin. Saponin-permeabilised parasites were incubated in different pH buffers in the presence of an ionophore, causing the pH of the parasite compartments to equilibrate with the pH of the buffers. A pH calibration curve was generated based on the ratio of the fluorescence intensity of FITC-dextran measured at two different wavelengths (530 nm and 585 nm). This standard curve was used for determination of pH of the parasite's digestive vacuole.

Next, the assay of 4-hour artemisinin pulse was performed for the assessment of parasite growth and viability. Mid ring stage parasites were pulsed for 4 hours (to mimic the drug's short half-life in human body) with different concentrations of artemisinin prepared by two-fold serial dilutions. After 4 hours, the parasite cultures were washed to remove the drug and incubated in normal culture conditions for additional 24 and 48 hours. The effects of the treatment were

evaluated at 24-hour post-treatment (to assess parasite growth and parasitaemia in the same cycle) and at 48-hour post-treatment (to examine the parasite viability in the next cycle) using SYBR Green I staining. The increase of parasitaemia calculated at 48-hour post-treatment represents the parasite viability. The percentage of parasite growth inhibition was measured based on the parasitaemia at 24- and 48-hour post-treatment for determination of the 4-hour pulse inhibitory concentration 50% ($IC_{50\text{-}4\ hours}$). The sub-lethal concentrations of artemisinin that caused less than 25% parasite death and affected the parasite growth were selected to be employed in the subsequent experiment.

In the experiment to measure the pH of the digestive vacuole, mid ring stage parasites in resealed erythrocytes with and without FITC-dextran were pulsed with sub-lethal concentrations of artemisinin for 4 hours. Like in the 4-hour artemisinin pulse assay, the parasite cultures were washed to remove the drug and further cultured for 24 and 48 hours. At 24-hour post-treatment, parasite with FITC-dextran-containing digestive vacuoles was isolated with saponin (0.035% w/v) for digestive vacuole pH measurement by flow cytometry. Parasite cultures using resealed erythrocytes without FITC-dextran were split into two aliquots before being used for the assessment of parasite growth at 24-hour post treatment and parasite viability at 48-hour post-treatment. The assay of 4-hour drug pulse with sub-lethal concentrations was also performed at mid trophozoite stage parasites to enable direct measurement of the digestive vacuole pH. The summarised flow for the study is illustrated in Figure 1.1.

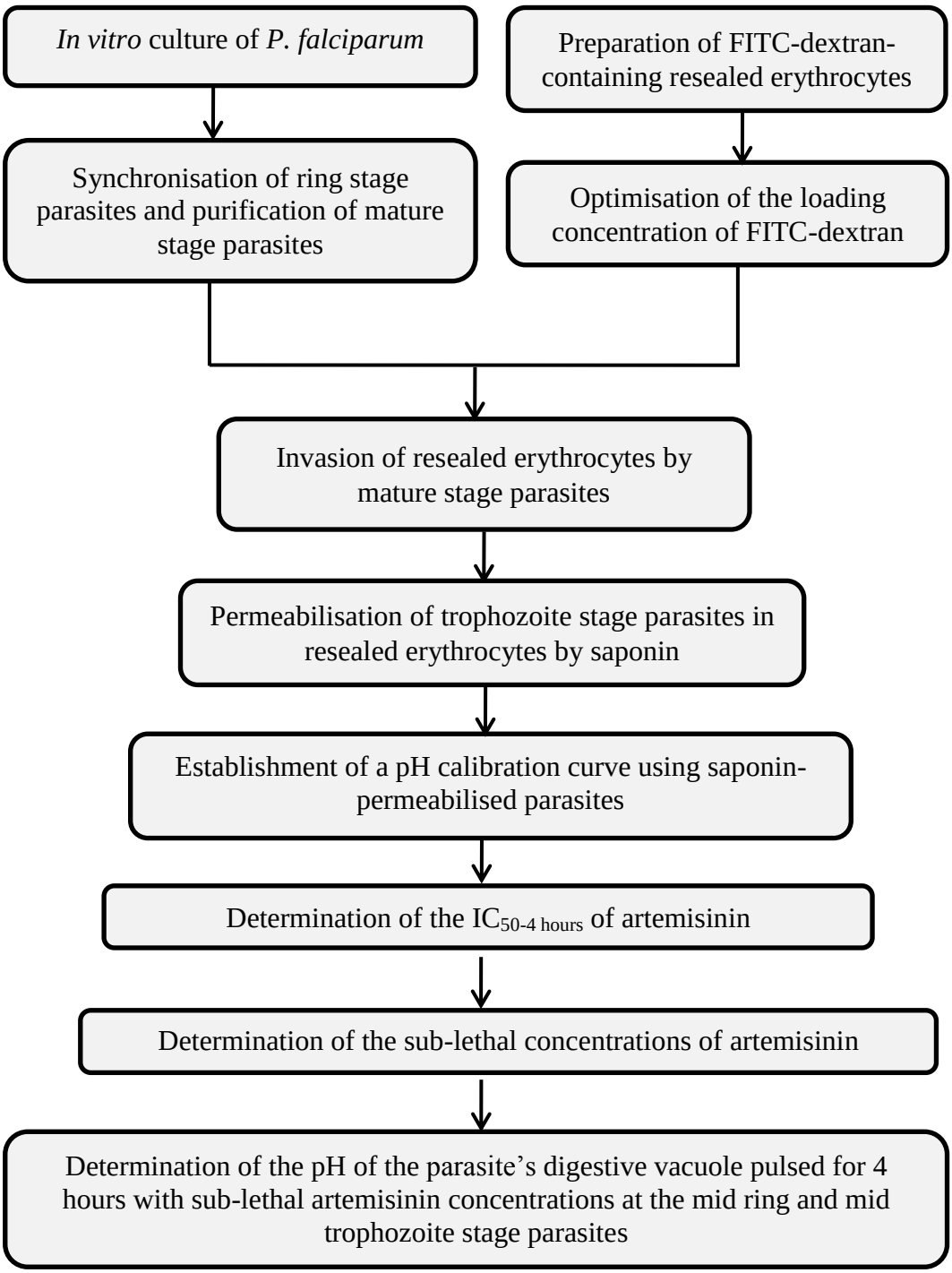

Figure 1.1: Flowchart of the experiments throughout the study

A pH calibration curve was established using the ratiometric pH indicator, FITC-dextran incorporated into the saponin-permeabilised parasites. The pH calibration curve was used to measure the digestive vacuole pH. The sub-lethal concentrations were determined in the assay of 4-hour artemisinin pulse. These concentrations were employed in the subsequent experiment using the same assay of 4-hour drug pulse to measure the pH of parasite's digestive vacuole.

CHAPTER 2

LITERATURE REVIEW

2.1 Overview of malaria

Malaria is a lethal infectious disease, which has been a scourge of humanity since ancient times. The causative agents of the disease are malaria parasites of the genus *Plasmodium* that can be transmitted by female mosquitoes of the genus *Anopheles*. After the discovery of the malaria parasite in the human erythrocyte in 1880 by Laveran (Hanboonkunupakarn and White, 2016), many studies have been extensively carried out as malaria has been widely spread throughout many countries in the world. Various strategies and efforts including the use of insecticide-treated bed nets, indoor residual spraying and antimalarial drugs have contributed to the control and elimination of the disease (Tizifa *et al.*, 2018). Due to the problem of drug resistance, malaria still remains a major health issue especially in Southeast Asia and other tropical regions in the world (Cui *et al.*, 2015).

2.2 Distribution of malaria

Malaria mostly occurs in tropical and sub-tropical countries where temperature, humidity and rainfall are relatively high and suitable for parasite growth and development within the mosquitoes (Kar *et al.*, 2014). To date, 91 countries have ongoing malaria transmission with most cases and deaths occur in Africa (WHO, 2018). According to WHO (2018), most malaria cases in 2017 were reported

in the African region with 200 million cases (92%) followed by the Southeast Asia region (5%) and the Eastern Mediterranean region (2%). Fifteen countries in sub-Saharan Africa and India were responsible for almost 80% of the malaria cases worldwide with five countries namely Nigeria (25%), Democratic Republic of the Congo (11%), Mozambique (5%), India (4%) and Uganda (4%) accounted for nearly half of the total malaria statistics worldwide (Figure 2.1).

In Malaysia, there has been a tremendous reduction in malaria burden in the past two decades (WHO, 2018). Even there was a fluctuation of malaria cases in 2005-2009 (Figure 2.2), the number of cases gradually decreased in 2010. The number of malaria cases in 2017 continually dropped to 508 cases including the cases of *P. vivax*, *P. falciparum* and imported cases. However, there was an increase of the total malaria cases in 2017 due to *P. knowlesi* infection. Sabah and Sarawak have contributed to the majority of *P. knowlesi* cases in Malaysia followed by several states in Peninsular Malaysia (Yong *et al.*, 2018).

2.3 Human malaria parasites

The phylum Apicomplexa comprises of diverse obligate intracellular parasites of the genus *Plasmodium, Babesia, Toxoplasma, Cryptosporidium, Eimeria* and *Theileria* (Reid, 2015). There are about 200 species of *Plasmodium* and five of them are identified to cause infection in human namely *P. falciparum, P. vivax, P. ovale, P. malariae* and *P. knowlesi* (Grossman *et al.*, 2017).

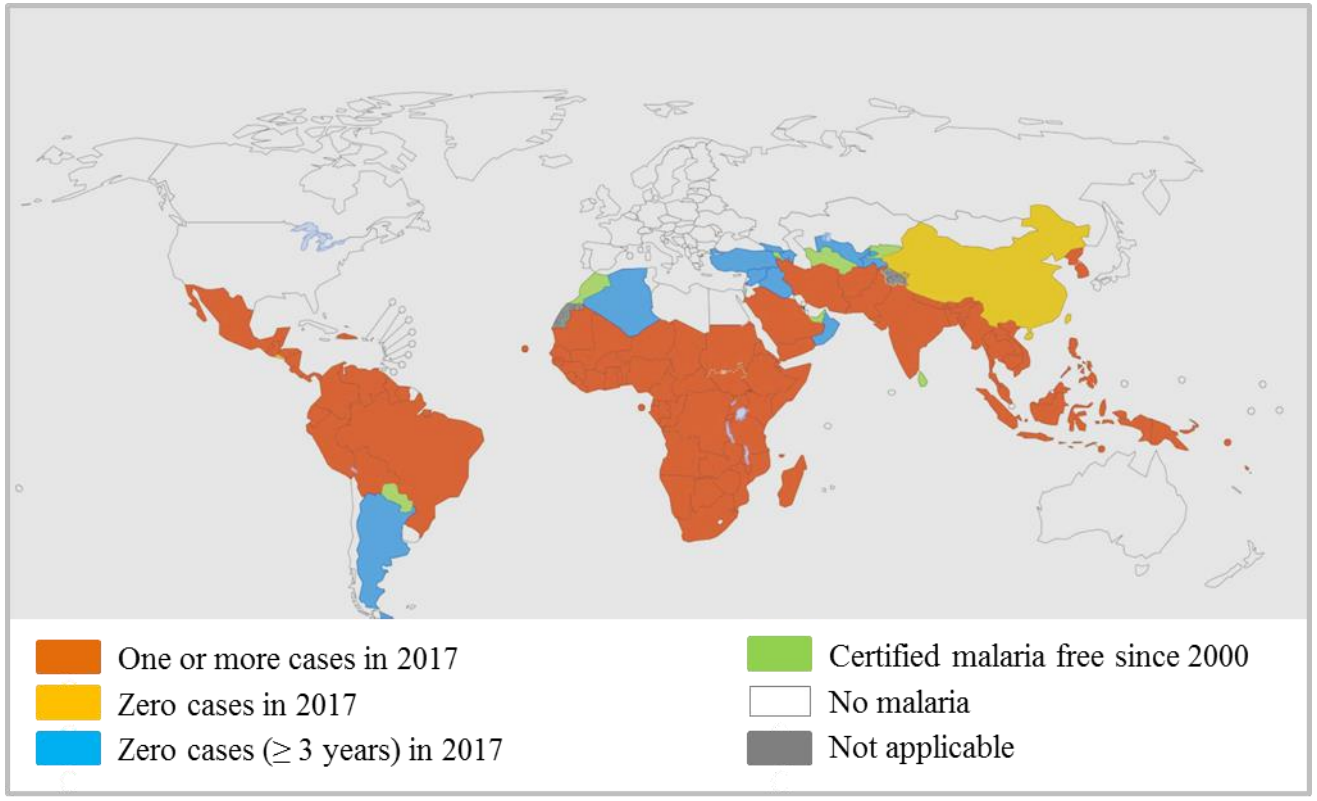

Figure 2.1: The malaria incidence rates worldwide from 2000-2017

All countries in the European region and China reported zero indigenous cases in 2017. Certain regions such as in Southeast Asia are still in active malaria transmission. Modified from World Malaria Report WHO (2018).

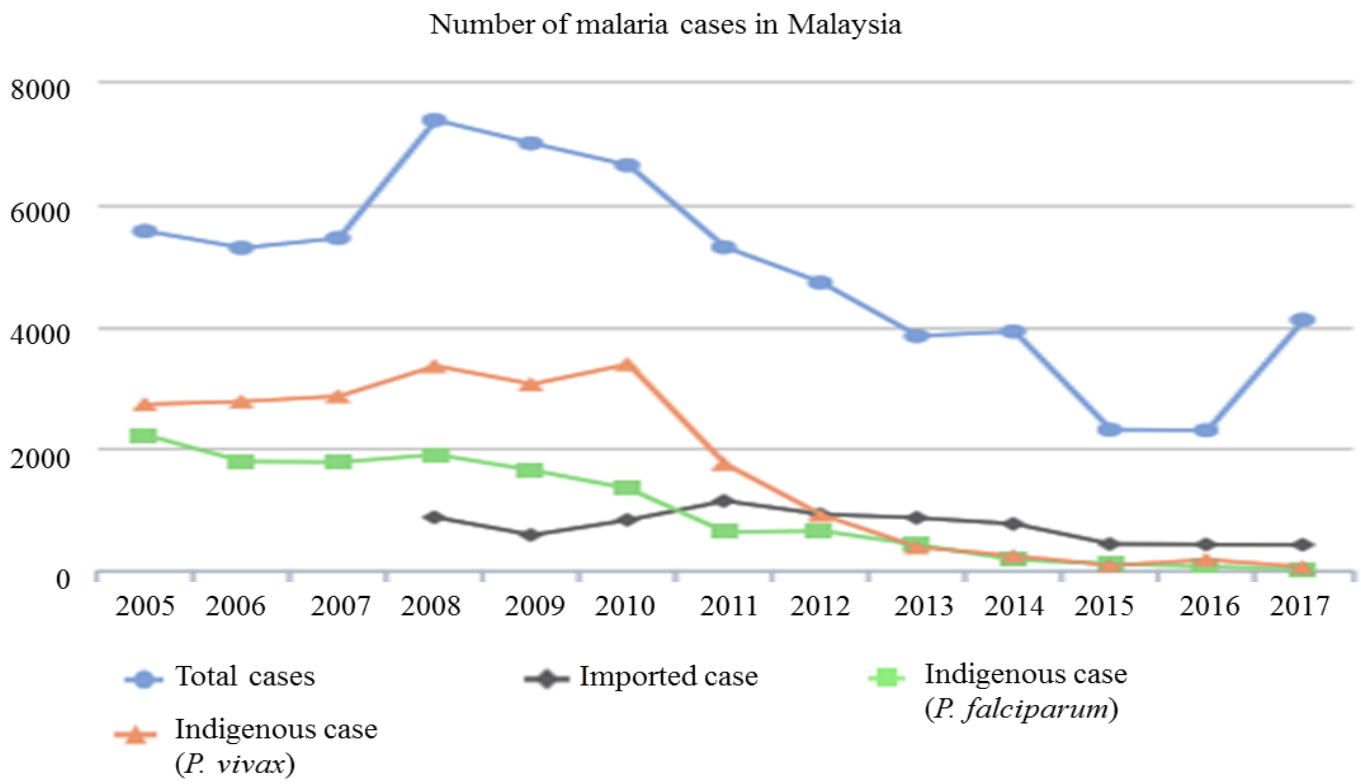

Figure 2.2: The number of malaria cases in Malaysia from 2005-2017

The number of malaria cases increased in 2008 with the highest cases was from *P. vivax.* The cases of *P. vivax* and *P. falciparum* decreased in the following years. In 2017, the total cases showed a slight increase due to the cases of *P. knowlesi.* Modified from WHO (2018).

Plasmodium knowlesi has been always misdiagnosed as *P. malariae* by microscopic examination. Now, the advancement of tools used for diagnosing malaria is able to differentiate the genetic components between these two species (Mohring *et al.*, 2019). *P. malariae* has the ability to persist in the intraerythrocytic stage for a long time, but does not cause a hypnozoite infection (Grossman *et al.*, 2017). The hypnozoites can be observed in *P. ovale* and *P. vivax* infections, which are able to remain dormant in the liver cells up to several months or years and can cause a relapse infection (Okafor and Finnigan, 2019).

Among the five human malaria parasites, *P. falciparum* is responsible for the vast majority of mortality and morbidity worldwide where it is predominantly distributed in sub-Saharan Africa (Howes *et al.*, 2016). *P. falciparum* is the most virulent malaria parasite that can cause high parasitaemia and able to invade host erythrocytes of different ages (Geleta and Ketema, 2016).

2.4 Life cycle of the malaria parasite

The malaria parasite has a complex life cycle that alternates between a sexual cycle in a mosquito vector and an asexual cycle in a human host.

2.4.1 Sexual cycle of the malaria parasite within a mosquito

The sexual cycle of the malaria parasite commences when a female mosquito ingests microgametocytes (male) and macrogametocytes (female) from an infected human during a blood meal (Figure 2.3) (Josling and Llinás, 2015).

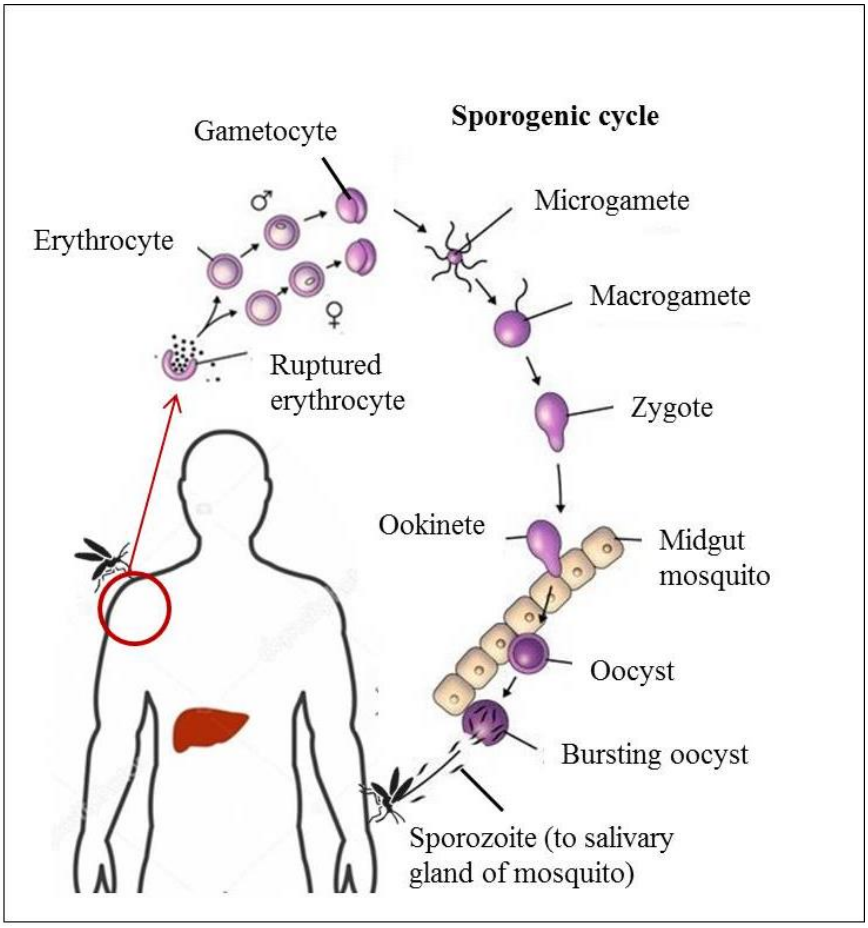

Figure 2.3: The sexual cycle of the malaria parasite within a mosquito

Microgametocytes (male) and macrogametocytes (female) are ingested by a mosquito during a blood meal and delivered to the mosquito's midgut. These gametocytes undergo maturation into microgametes and macrogametes. The microgametes fuse with the macrogametes forming zygotes, which undergo meiosis to form ookinetes. The ookinetes penetrate the midgut wall and mature into oocysts. The oocysts rupture releasing numerous sporozoites, which migrate to the salivary gland allowing infection of a new host during the blood meal. Modified from Karunamoorthi (2014).

Exflagellation of the microgametocytes leads to the production of eight microgametes, which can fuse with macrogametes to produce zygotes in the mosquito's midgut. The zygotes undergo meiosis to form motile ookinetes, which penetrate the midgut wall and differentiate into oocysts. After ten days of maturation, the oocysts rupture releasing numerous sporozoites. The sporozoites travel to the salivary gland where they are ready to be transmitted to a human during another blood meal.

2.4.2 Asexual cycle of the malaria parasite within a human

The asexual cycle of the malaria parasite begins when a mosquito inoculates sporozoites into a human during a blood feeding. The sporozoites enter the blood circulation and invade the liver cells to initiate the exoerythrocytic cycle (Figure 2.4A) (Josling and Llinás, 2015). Inside the liver cell, the parasite multiplies and matures into a schizont. The schizont ruptures releasing numerous merozoites. The exoerythrocytic cycle takes place between 2-7 days depending on the species of the malaria parasite (Bertolino and Bowen, 2015). The merozoites enter the blood circulation and invade the erythrocytes to initiate the intraerythrocytic cycle (Figure 2.4B). Inside the erythrocyte, the parasite develops into three distinct stages; ring, trophozoite and schizont.

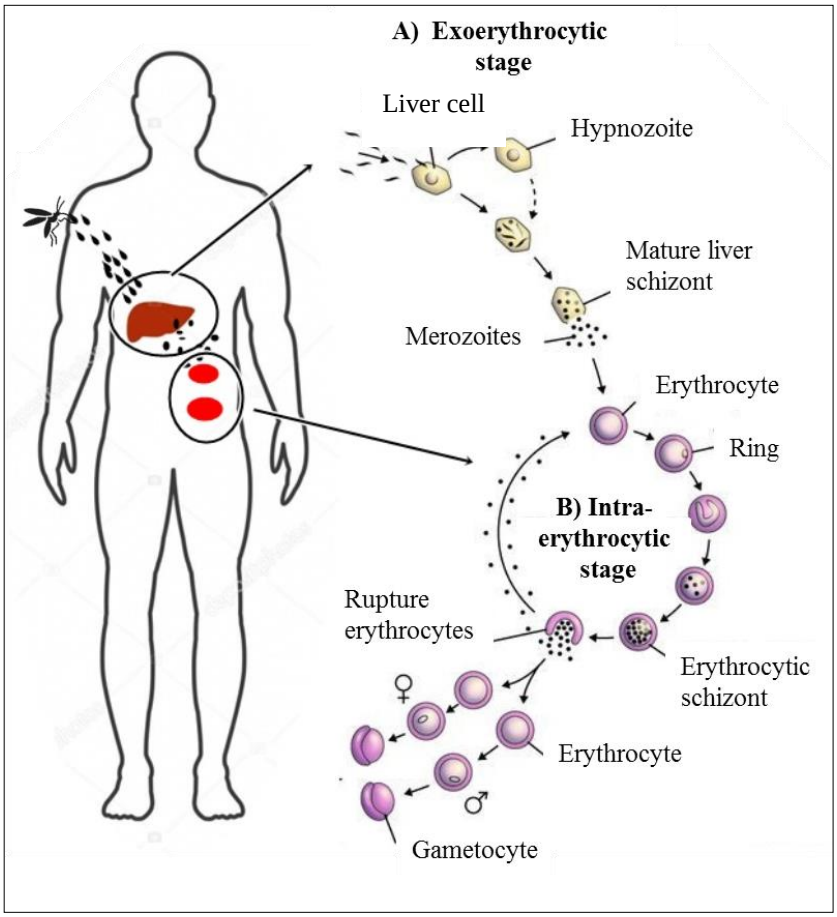

Figure 2.4: The asexual cycle of the malaria parasite within a human

(A) Sporozoites inoculated by an infected mosquito enter the liver cells of a human host to begin the exoerythrocytic stage. The parasites mature into schizonts, which burst to release thousands of merozoites. (B) The intraerythrocytic stage is initiated after the merozoites invade erythrocytes. The parasites mature into ring, trophozoite and schizont stages. The mature schizonts burst to release merozoites, which reinvade new erythrocytes and repeat the same cycle. Some of the merozoites differentiate into male and female gametocytes that can be ingested by a mosquito thus completing the life cycle. Modified from Karunamoorthi (2014).

In the early ring stage, the central region of the parasite is quite thin, while the peripheral region is thicker and contains nucleus and other organelles (Poostchi *et al.*, 2018). This gives its characteristic ring appearance in Giemsa-stained blood smears (Figure 2.5A). The ring stage of *P. falciparum* lasts for 24 hours from the time of merozoite invasion during which the metabolic activity and DNA levels are relatively low (Wallqvist *et al.*, 2016). In the trophozoite stage, the parasite rapidly grows with an increase in the metabolic activity and RNA levels (Wallqvist *et al.*, 2016). The parasite becomes globular with an enlarged cytoplasm where the digestive vacuole is readily observed by the accumulation of haemozoin pigment (Figure 2.5B). The trophozoite stage lasts for 10-12 hours in duration (25-38 hour post-invasion). The trophozoite progresses to the schizont stage (38-48 hour post-invasion) (Figure 2.5C) and undergoes multiple rounds of mitotic DNA replication to produce 16-20 merozoites that are capable of invading new erythrocytes (De Niz *et al.*, 2016).

The rapid growth and development within the erythrocytes require the parasites to obtain nutrients and metabolise various biological molecules in order to survive and reproduce (Abshire *et al.*, 2017). A better understanding of the parasite's metabolisms such as haemoglobin metabolism may lead to the development of novel therapeutic strategies, which exploits the uniqueness of the parasite (Lechuga *et al.*, 2019).

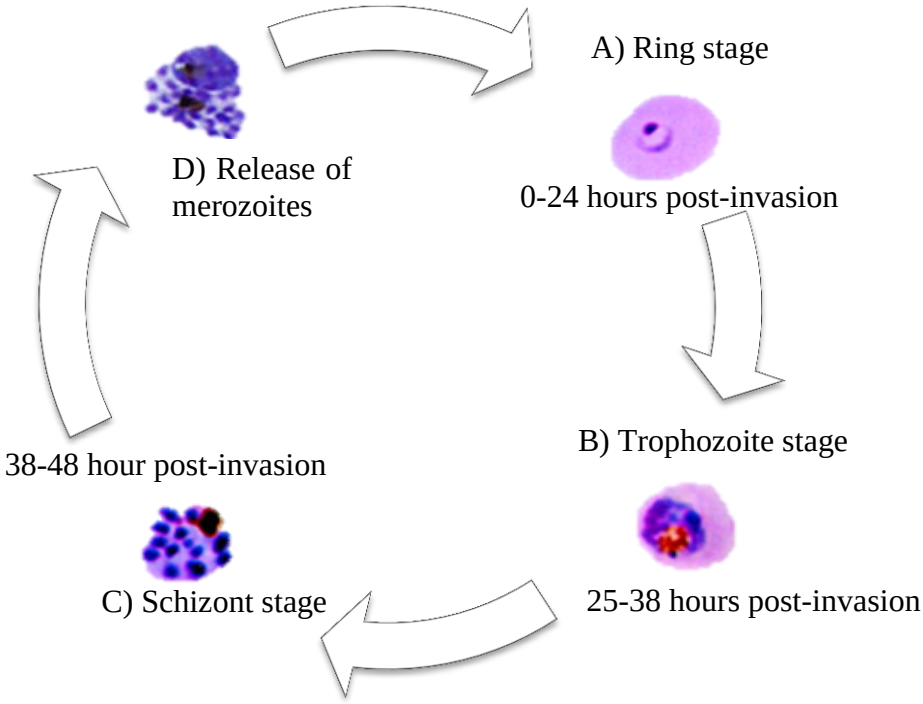

Figure 2.5: The intraerythrocytic stages of *P. falciparum*

(A) After invasion, the ring stage parasite lasts for 24 hours before grow to (B) the trophozoite stage. The parasite becomes enlarged and globular with the appearance of haemozoin in the digestive vacuole. This stage lasts for 25-38 hours post-invasion before develop to (C) the schizont stage (38-48 hours post-invasion) where nuclear division occurs to produce a multinucleated schizont. The schizont ruptures releasing numerous merozoites, which will invade new erythrocytes to repeat the same intraerythrocytic cycle.

2.5 Haemoglobin metabolism within the malaria parasite

The malaria parasite internalises a large portion of the cellular content of its host erythrocyte (Sigala and Goldberg, 2014). The internalised cytoplasm consisting largely of haemoglobin is transported to the digestive vacuole (Milani *et al.*, 2015) where it is digested to provide amino acids for protein synthesis (Jonscher *et al.*, 2019) and space for growth (Wendt *et al.*, 2016).

2.5.1 Haemoglobin ingestion by the malaria parasite

The malaria parasite ingests the erythrocyte cytoplasm in spite of being enclosed within the parasitophorous vacuole (PV) (Santi-Rocca and Blanchard, 2017). During the early ring stage of development, the haemoglobin ingestion is thought to be limited (Heller and Roepe, 2018). When the parasite enters the mid ring stage, small portions of the erythrocyte cytoplasm are taken up by micropinocytosis (Abu Bakar *et al.*, 2010; Xie *et al.*, 2016) . This process involves structures called cytostomes that are formed by double-membrane invaginations of the parasitophorous vacuolar membrane (PVM) and the parasite plasma membrane (PPM) (Figure 2.6A) (Milani *et al.*, 2015). The protein composition of cytostomes is not known, but it has been shown that the endocytic process is mediated by actin (Jonscher *et al.*, 2019; Lazarus *et al.*, 2008). As the parasite matures to the trophozoite stage, a larger volume of haemoglobin is ingested by cytostomes (Abu Bakar *et al.*, 2010; Wendt *et al.*, 2016). There is evidence for continuing haemoglobin uptake by the schizont stage parasite (Josling and Llinás, 2015) as it

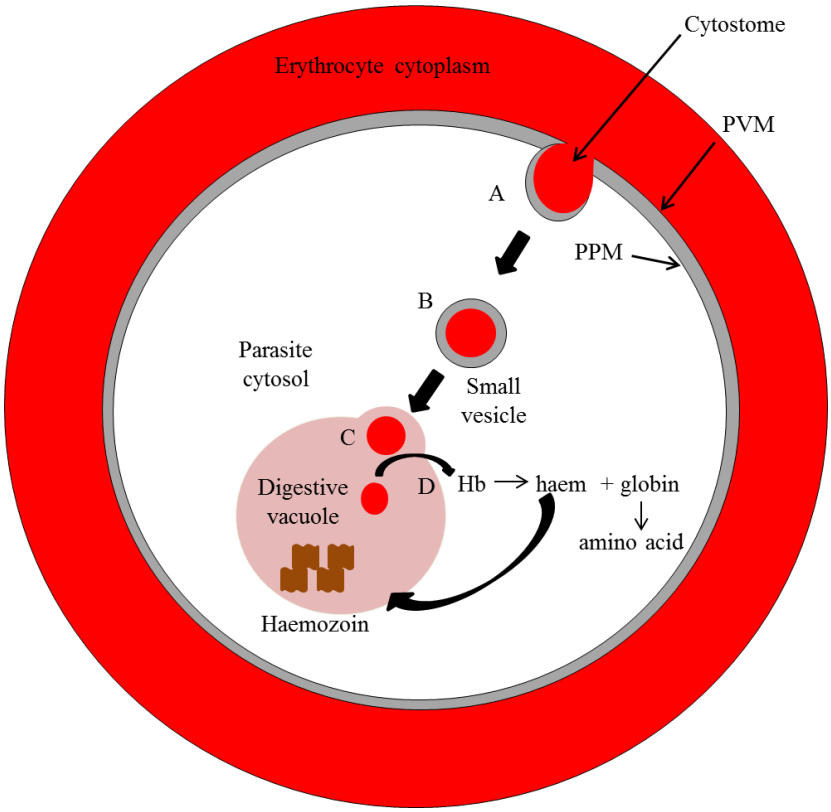

Figure 2.6: The schematic diagram of haemoglobin ingestion, transport to and digestion in the digestive vacuole of *P. falciparum*

(A) Haemoglobin is internalised by the parasite via a cytostome. (B) The budding of the cytostome forms a double-membrane vesicle, which is directly transported to the digestive vacuole. (C) The outer membrane of the vesicle fuses with the digestive vacuole releasing haemoglobin. (D) Haemoglobin is degraded to amino acids and a toxic by-product haem. Haem is detoxified to an inert polymer known as haemozoin by the process of biocrystallisation. PVM: parasitophorous vacuolar membrane, PPM: parasite plasma membrane, Hb: haemoglobin. Modified from Abu Bakar *et al.* (2010).

eventually consumes 80% of the erythrocyte haemoglobin and occupies most of the erythrocyte volume (Silva *et al.*, 2017).

Other distinct mechanisms that mediate the haemoglobin uptake have been proposed (Elliott *et al.*, 2008; Medeiros *et al.*, 2012; Wendt *et al.*, 2016). The early ring stage parasite was thought to fold around a big gulp of the erythrocyte cytoplasm to take up haemoglobin. This endocytic process was continued by small cytostome-derived haemoglobin-containing vesicles and tubules as the parasite matures. Additional cytostome-independent endocytic structures called phagosomes were described in more mature stage parasites. On the other hand, another study proposed that extended cytostomal tubes were used by the parasite to internalise and transfer haemoglobin to the digestive vacuole via a vesicle-independent process (Lazarus *et al.*, 2008). However, live-cell imaging and photobleaching technique to investigate the dynamics and connectivity of different endocytic compartments did not support the role of the macropynocytic event in the parasite (Abu Bakar *et al.*, 2010; Liu *et al.*, 2019).

2.5.2 Haemoglobin transport to the digestive vacuole

In the late ring stage of development, haemoglobin transport commences after cytostomes pinch off at the neck forming double-membrane, haemoglobin-containing vesicles (Klemba *et al.*, 2004; Milani *et al.*, 2015) (see Figure 2.6B). The transport of haemoglobin-containing vesicles has been demonstrated to utilise an actin-myosin motor system (Milani *et al.*, 2015). The haemoglobin and inner membrane of the vesicles have been shown to be digested by proteases and

phospholipases, respectively en route to the digestive vacuole (Abu Bakar *et al.*, 2010; Burda *et al.*, 2015). The outer membrane of the vesicles has been reported to fuse with the plasma membrane of the digestive vacuole (Milani *et al.*, 2015) (see Figure 2.6C), resulting in the delivery of single-membrane, haemoglobin-filled vesicles into the lumen of the digestive vacuole (Jonscher *et al.*, 2019). A knockout of the gene encoding the *P. falciparum* digestive vacuole's aspartic protease, plasmepsin IV (*Pf*PM4) caused abundant accumulation of electron-dense vesicles in the digestive vacuole (Liu *et al.*, 2015). Once the digestive vacuole is fully formed, it appears to be the primary site of haemoglobin degradation and haem detoxification

2.5.2(a) The digestive vacuole of the malaria parasite

The digestive vacuole is formed de novo after each round of infection of the erythrocyte by the malaria parasite (Wendt *et al.*, 2016). The lack of the typical lysosomal acid phosphatase and glycosidases (Coronado *et al.*, 2014) has proved that the digestive vacuole of the malaria parasite is a specialised organelle that evolves to efficiently digest haemoglobin (Deshpande and Kuppast, 2016). The digestive vacuole has also been observed in other parasites such as in *Babesia caballi* and *Theileria equi* (Maji, 2018).

Microscopically, the alteration of the density of the digestive vacuole indicates that haemoglobin digestion has occurred (Wendt *et al.*, 2016). This process produces an insoluble toxic waste product called haem, which is detoxified by the formation of haematin dimers that biocrystallise to a chemically inert malaria pigment known as haemozoin (Xie *et al.*, 2016). Haemozoin can be observed by light

and electron microscopy as it is a very dense structure and lined up along a single axis in the parasite (Figure 2.7). Lipid bodies, whose contents are possibly derived from the digestive vacuole's wall and interior as well as the inner membrane of the transport vesicles, are also found adjacent to the digestive vacuole (Olafson *et al.*, 2015). These neutral lipid bodies have been suggested to promote haematin formation (Olafson *et al.*, 2015) and histidine-rich protein II (HRPII) (Gupta *et al.*, 2017).

2.5.3 Haemoglobin digestion in the digestive vacuole

In the digestive vacuole, haemoglobin that comprises of 95% of the cytosolic erythrocyte protein is digested by proteases via an ordered process (see Figure 2.6D) (Liu, 2017a). Haemoglobin has been initially digested by aspartic proteases (plasmepsins) and cysteine proteases (falcipains) into haem and globin (Coronado *et al.*, 2014). Globin has been further hydrolysed by metalloprotease (falcilysin) to release amino acids for incorporation into parasite proteins as the parasite has a restricted capability to synthesise amino acids de novo (Pandey and Pandey-Rai, 2015). The inhibition of plasmepsins and falcipains by a combination of the aspartic protease inhibitor, pepstatin and the cysteine protease inhibitor, E-64 was led to the accumulation of undigested haemoglobin indicating a complete inhibition of haemoglobin digestion (Klonis *et al.*, 2011; Milani *et al.*, 2015). Haemoglobin digestion is also crucial to create space for parasite growth and to generate osmolytes to prevent premature lysis of the erythrocytes (Kumari *et al.*, 2019). Like in lysosomes of mammalian cells and yeast vacuoles, pH homeostasis of the digestive